Biochimica et Biophysica Acta 1843 (2014) 234–244

Contents lists available at ScienceDirect

Biochimica et Biophysica Acta

journal homepage: www.elsevier.com/locate/bbamcr

Valvular dystrophy associated filamin A mutations reveal a new role of its first repeats in small-GTPase regulation

D. Duval [a,1], A. Lardeux [a,1], T. Le Tourneau [a], R.A. Norris [b], R.R. Markwald [b], V. Sauzeau [a], V. Probst [a], H. Le Marec [a], R. Levine [c], J.J. Schott [a], J. Merot [a,*]

[a] Institut du Thorax, INSERM UMR1087, CNRS UMR 6291, 8 Quai Moncousu 44007 Nantes Cedex, France
[b] Department of Regenerative Medicine and Cell Biology, Cardiovascular Developmental Biology Center, Children's Research Institute, Medical University of South Carolina, 171 Ashley Avenue, Charleston, SC 29425, USA
[c] Noninvasive Cardiac Laboratory, Department of Medicine, Massachusetts General Hospital, Boston, MA 02114, USA

ARTICLE INFO

Article history:
Received 10 July 2013
Received in revised form 26 October 2013
Accepted 28 October 2013
Available online 4 November 2013

Keywords:
Mitral valve prolapse
Filamin A
Rac1
RhoA
FilGAP

ABSTRACT

Filamin A (FlnA) is a ubiquitous actin binding protein which anchors various transmembrane proteins to the cell cytoskeleton and provides a scaffold to many cytoplasmic signaling proteins involved in actin cytoskeleton remodeling in response to mechanical stress and cytokines stimulation. Although the vast majority of FlnA binding partners interact with the carboxy-terminal immunoglobulin like (Igl) repeats of FlnA, little is known on the role of the amino-N-terminal repeats. Here, using cardiac mitral valvular dystrophy associated FlnA–G288R and P637Q mutations located in the N-terminal Igl repeat 1 and 4 respectively as a model, we identified a new role of FlnA N-terminal repeats in small Rho-GTPases regulation. Using FlnA-deficient melanoma and HT1080 cell lines as expression systems we showed that FlnA mutations reduce cell spreading and migration capacities. Furthermore, we defined a signaling network in which FlnA mutations alter the balance between RhoA and Rac1 GTPases activities in favor of RhoA and provided evidences for a role of the Rac1 specific GTPase activating protein FilGAP in this process. Together our work ascribed a new role to the N-terminal repeats of FlnA in Small GTPases regulation and supports a conceptual framework for the role of FlnA mutations in cardiac valve diseases centered around signaling molecules regulating cellular actin cytoskeleton in response to mechanical stress.

1. Introduction

The Filamin gene family consists of three highly related homologous proteins produced from three separate gene loci. Filamin's A (alpha), B (beta), and C (gamma) share similar molecular organization consisting of a conserved N-terminal actin binding region followed by 24 immunoglobulin-like (Igl) repeated domains among which the 24th is involved in non-covalent protein dimerization [1–3]. Filamin A (FlnA) is the first actin filament cross-linking protein identified in non-muscle cells and organizes actin filaments in orthogonal networks to stabilize the cellular actin cortex [4].

Many previous studies defined central roles for FlnA in mechanoprotection, cell adhesion, spreading and migration [1–3,5,6], cell survival, morphogenesis, wound healing and human disease pathogenesis [6,7]. In addition to its interactions with actin, FlnA functions also depend on its cell and tissue-specific association with numerous binding partners. To date, over 90 FlnA-binding partners have been identified many of which participate in the regulation of intracellular signaling pathways to promote cytoskeleton remodeling. Some of these partners include small GTPases and their regulators, integrins receptors and associated kinases [3,8]. Although the structural features underlying the binding of specific partners to the C-terminal Igl repeats are becoming better understood, there is a paucity of information regarding functional determination of the N-terminal FlnA region for which few protein partners have been identified [9–11]. One that does interact with the 3rd Igl repeat of N-terminal FlnA is R-Ras which is known to participate in the maintenance of endothelial cell barrier function [12,13]. The intermediate filament protein vimentin and PKCε which participate in cell adhesion also interact with FlnA 1–8 repeats whereas the tyrosine kinase Syk binds the fifth repeat of FlnA and participates in platelet activation [11,14,15].

Human mutations in the *FLNA* gene cause a wide spectrum of congenital anomalies including: periventricular heterotopy (PVH), Melnick–Needles syndrome (MNS), otopalatodigital syndrome (OPD), and myxomatous valvular dystopohy [16–18]. Causal FlnA mutations that contribute to each of these diseases are found throughout the encoded protein, further suggesting tissue-specific function of the affected FlnA subdomains. Whereas mutations that cause PVH, MNS,

* Corresponding author. Tel.: +33 2 28 08 01 64.
E-mail addresses: damien.duval@etu.univ-nantes.fr (D. Duval), aurelie.lardeux@gmail.com (A. Lardeux), thletourneau@yahoo.fr (T. Le Tourneau), norrisra@musc.edu (R.A. Norris), markwald@musc.edu (R.R. Markwald), vincent.sauzeau@inserm.fr (V. Sauzeau), vincent.probst@chu-nantes.fr (V. Probst), herve.lemarec@univ-nantes.fr (H. Le Marec), RLEVINE@PARTNERS.ORG (R. Levine), jjschott@univ-nantes.fr (J.J. Schott), jean.merot@univ-nantes.fr (J. Merot).
[1] *D.D., and A.L. equally contributed to this work.

0167-4889/$ – see front matter © 2013 Elsevier B.V. All rights reserved.
http://dx.doi.org/10.1016/j.bbamcr.2013.10.022

and OPD are clustered primarily in the well-studied C-terminus of FLNA, myxomatous valvular dystrophy is caused by mutations in the poorly studied N-terminus. In the present study, we have analyzed the functional effects of two N-terminal mutations (FlnA–G288R and P637Q) that cause X-linked myxomatous valvular dystrophy (XMVD) [19,20]. We demonstrate that these mutations alter the balance of the small GTPases, RhoA and Rac1, and alter their potential to remodel the actin cytoskeleton during cell adhesion, spreading and migration and present candidate mechanisms by which this may contribute to the pathogenesis of mitral valve prolapse.

2. Materials and methods

2.1. Reagents

Polyclonal antibodies for GAPDH (1:10,000); RhoA (1:500) and HRP-conjugated antibodies (1:10 000) were purchased from Santa Cruz. Alexa Fluor 488 and Alexa Fluor 594 were purchased from Life Technologies. Monoclonal antibodies were purchased from Chemicon (anti-filamin A, 1:1000), BD Transduction Laboratories (anti-Rac1, 1:500), Sigma-Aldrich (FilGAP, 1:250; ß-actin, 1:500), Roche (anti-HA, 1:1000), Clontech (GFP, 1:1000). Y27632 and NSC23766 were purchased from Santa Cruz and human plasma Fibronectin from Sigma-Aldrich.

2.2. Cell culture, stable cell lines and transfection

The FlnA-deficient human melanoma cell line (M2) and the stably FlnA–WT transfected subclone (A7) were obtained from Dr. F Nakamura (Harvard University, Cambridge, MA) and shRNA knockdown HT1080 from Dr Calderwood (Yale University, New Haven, USA) [21]. M2 cells were cultured in minimum essential medium α (MEMα) supplemented with 8% newborn calf serum, 2% fetal calf serum (FCS) and HT1080 cells in DMEM supplemented with 10% FCS and 2 μg/ml puromycin. To establish stable cell lines expressing FlnA–WT, G288R and P637Q, M2 cells were transfected with pcDNA3–FlnA–WT, pcDNA3–FlnA–G288R and pcDNA3–FlnA–P637Q plasmids using Fugene6 (Roche-Applied Science). The clones were selected and then grown in the presence of G418 (800 μg/ml for selection and 200 μg/ml for routine culture).

2.3. Plasmid and SiRNA

FlnA–WT cDNA was cloned in pcDNA3 and G288R or P637Q mutations introduced using QuikChange® Site-Directed Mutagenesis Kit (Stratagene). GFP tagged shRNA resistant FlnA–WT cDNA was a kind gift of Dr D Calderwood (Yale University, New Haven CT, USA) in which G288R and P637Q were introduced by site directed mutagenesis [21]. The pCMV5 HA–FilGAP WT was a gift of Dr Yasutaka Ohta (Division of Cell Biology, Kitasato University, Kitasato, Japan). To deplete endogenous FilGAP, siRNA oligonucleotide duplexes targeting the sequence 5′-AAGATAGAGTATGAGTCCAGGATAA-3′ (nt 1975–1999 of FilGAP) were used [22]. Control siRNA duplexes targeting GFP were used (sense 5′-GCAAGCUGACCCUGAAGUUCAU-3′, antisense 5′-GAACUUCAGGGU CAGCUUGCCG-3′). The cells were transfected according to the suppliers' guidelines (Eurogentec) and used 48 hours post transfection.

2.4. Adhesion and spreading assays

In adhesion assays, 2.5×10^4 cells were seeded on coverslips coated with 25 μg/ml fibronectin and incubated at 37 °C for 45 min followed by two consecutive PBS washes. Adherent cells were fixed with 2% paraformaldehyde (PFA), stained with DAPI and counted in 10 fields under microscopic observation (10× objective). Alternatively, the impedance measurement technology of the xCELLigence system was used to monitor cell adhesion and spreading [23]. 1×10^4 cells per well were plated into 96-wells E-Plates (Roche Diagnostics, GmbH), placed on the Real Time Cell Analyzer and incubated at 37 °C in a 5% CO_2 incubator. Cell adhesion and spreading were measured as the changes in the electrical impedance between the microelectrodes lining the bottom of the wells and expressed as a *Cell Index* (CI) according to the manufacturer's guidelines. For inhibitor assays, Y27632 (10 μm) and NSC23766 (10 μm) were added to the culture medium when the cells were seeded in the 96-wells E-Plate. Impedance measurements were taken every 1 min for 3 hours. The slope of CI changes (dCI/dt) was calculated between $t_{30\text{min}}$ and $t_{1\text{h}30\text{min}}$.

2.5. Migration assays: wound healing and "Transwell" assays

In wound healing assays, confluent cell monolayers were scratched with a pipette tip, washed with phosphate-buffered saline (PBS) and cell migration monitored using a Leica DMI6000B microscope equipped for time-lapse video microscopy. Wound closure was monitored for 24–28 h on 3 fields per well and the data are presented as % of closure of FlnA–WT cells monolayer wound closure at $t = 24$ hrs. Transwell migration assays were performed using 8 μm pore size bottom filter chambers (Corning, Costar Corp). 5×10^4 cells were serum-starved overnight and seeded in 200 μl of serum-free MEM into the upper chamber, whereas the lower compartment was filled with MEM supplemented with 10% serum. After 8 hours at 37 °C, cells remaining on the upper surface of the filter were wiped out with a cotton swab, and the cells that had migrated on the lower surface of the filter were fixed, stained with DAPI and counted in ten microscopic fields.

2.6. Immunofluorescence microscopy

Cells were seeded on coverslips, washed three times with PBS and subsequently fixed in 2% PFA for 15 min, permeabilized with 0.1% Triton X-100, incubated with primary antibodies (dilution: 1/1000) in 1% of bovine serum albumin for 1 h and then with Alexa 594 or 488 conjugated secondary antibody for 1 h. Rhodamine conjugated-phalloidin (1 μg/ml, Invitrogen) was added for 20 min to detect actin cytoskeleton and nuclei were counterstained with DAPI for 10 min. Coverslips were mounted in Prolongold (Invitrogen) and observed on a Zeiss Axiovert microscope.

2.7. Co-immunoprecipitation and immunoblotting

Cells transfected with FilGAP-HA were lysed in NETF buffer containing: 100 mM NaCl, 2 mM EGTA, 50 mM Tris pH 7.5, 50 mM NaF, 1% NP-40, 1 mM PMSF, 1 mM Na_3VO_4, 1× protease inhibitor cocktail (Roche) and lysates clarified by centrifugation (15,000 ×g for 15 min at 4 °C). The cell lysates (500 μg) were incubated with 6 μg of anti-HA for 2 h at 4 °C and then with 30 μl of protein A conjugated beads (Dynabeads, Invitrogen) for 1 h at 4 °C. The immunoprecipitates were washed four times with NETF buffer and separated by SDS-PAGE transferred to nitrocellulose membrane (Bio-Rad Transblot). Immunoblots probed with appropriate antibodies and revealed using enhanced chemiluminescence kit (GE Healthcare). Chemiluminescence signals were quantified using an Imager system (Roche Diagnostic) and the data normalized with respect to GAPDH.

2.8. Glutathione-S-transferase (GST) protein purification and GST pull-down

GST–Rothekin (GST–RTK) or GST–Crib containing the Cdc42/Rac Interactive Binding (Crib) region of p21 activated kinase were produced in Bl21 *E. coli* treated overnight with 1 mM IPTG at 25 °C. The GST–Rac1–Q61L fusion protein used to analyze FilGAP activity in a Rac1–GAP activity pull down assay, was a kind gift of Dr C. Guilluy and K Burridge (Institut du Thorax, Nantes, France) [24]. The GST-fusion proteins were purified using Glutathione Agarose 4B beads (Macherey-Nagel). Cells grown for 2–4 hrs after seeding were lysed in NETF buffer. The cell lysates were centrifuged at 15,000 ×g for 15 min at 4 °C. 500 μg of cleared cell lysates were incubated with GST-tagged

proteins (30 μg) and rotated (18 rpm) for 1 h at 4 °C. The beads were washed four times with cell lysis buffer and bound proteins separated by SDS-PAGE. Bound Rac1 and RhoA were detected by immunoblotting as describe above. In Rac1–GAP activity assay, FlnA–WT, G288R and P637Q stable cell lines were transfected with FilGAP–HA and pulled down FilGAP quantified by western blotting.

2.9. Statistical analysis

Each assay presented here was performed at least three times. Graphs depict mean values ± SEM of sample size *n*. Images presented here are representative of each sample analyzed. Data were analyzed using Prism (GraphPad Software) and *P*-values were generated using

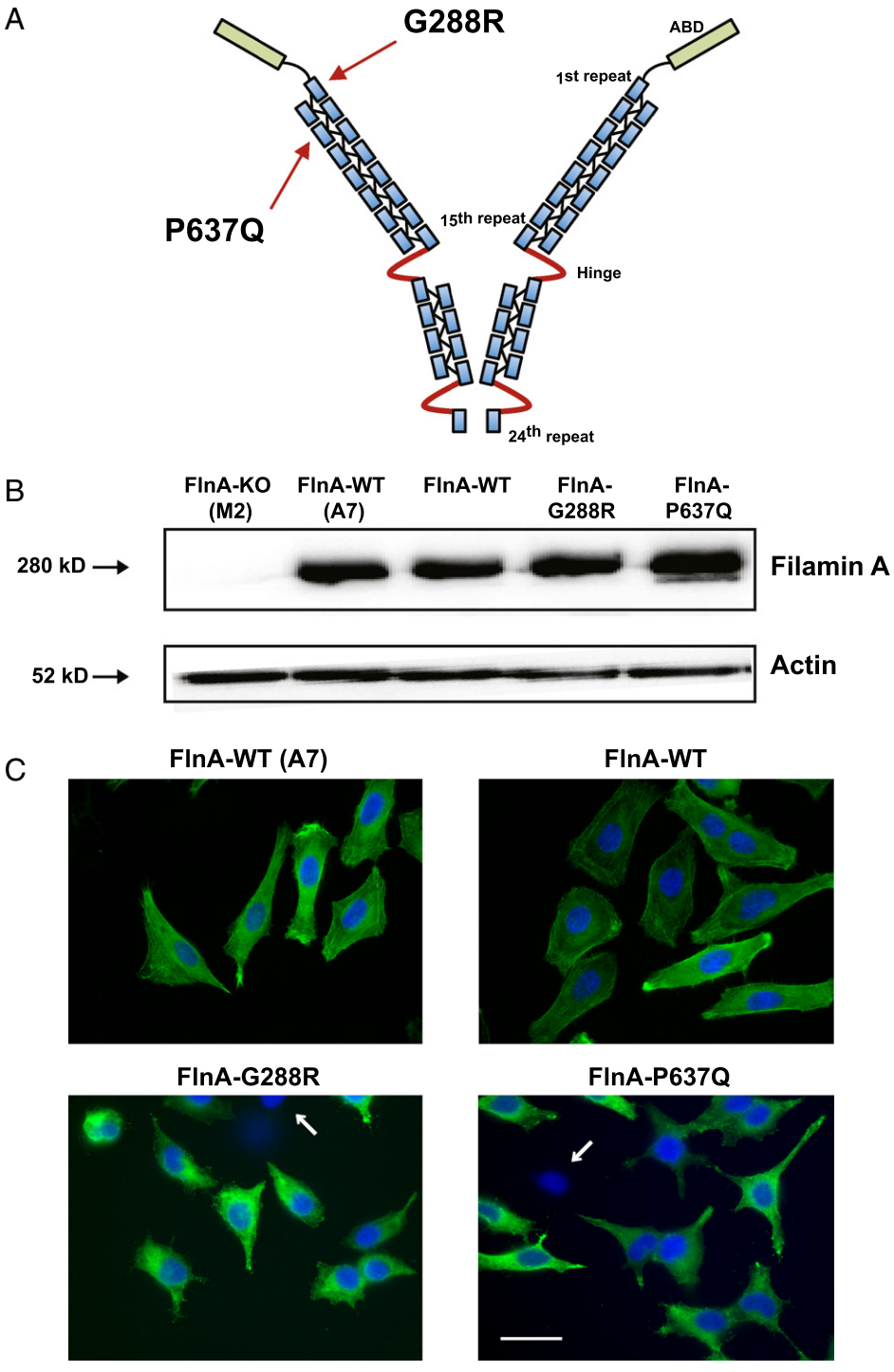

Fig. 1. Screening of stable melanoma cell lines expressing FlnA-WT, G288R or P637Q. A. Schematic representation of human Filamin A. The N-terminal actin-binding domain (ABD) is followed by 24 Igl repeats. The Igl repeats are interrupted by two hinges regions (in red). FlnA–G288R and P637Q mutations associated to dystrophy valvular are located on repeats 1 and 4, respectively. B. Western blot analysis of total cell extracts (25 μg) from original M2 (FlnA-deficient), A7, FlnA–WT, G288R and P637Q cell lines. Only clones with a FlnA/actin expression ratio comparable to the original A7 cell line were conserved. C. Selection of FlnA stable cell lines: Immunostaining of the original FlnA–WT expressing cell line A7 (upper left) and those established in the present study FlnA–WT (upper right), G288R and P637Q (lower images) (anti-FlnA antibody, green). Only clones exhibiting over 80% of FlnA positive cells were selected and the arrows indicate the few non-expressing cells in mutant FlnA clones. The nuclei were stained with DAPI (blue) (scale bar: 20 μm).

a Mann–Whitney test or two-way ANOVA test: $^{*}P < 0.05$; $^{**}P < 0.01$; $^{***}P < 0.001$.

3. Results

3.1. FlnA mutants restore mesenchymal morphology of FlnA deficient melanoma cells

The FlnA-deficient melanoma cell line (M2) is a tractable cell line for analyzing the function of the two FlnA mutations (G288R and P637Q) and is commonly used as a model to study FlnA effects on cell behavior (Fig. 1A) [25]. We thus established cell lines stably expressing FlnA–G288R or FlnA–P637Q. In addition, to avoid any bias linked to the use of a FlnA plasmid construct different from that used to establish the original FlnA–WT-reconstituted cell line (A7), we also established FlnA–WT stable cell lines [25]. As illustrated in Fig. 1B and C, only clones exhibiting over 80% of FlnA positive cells and a FlnA/ß-actin ratio comparable to that of the wild-type melanoma cell line (A7) were selected. Three clones of each FlnA construct were amplified and further analyzed. They gave similar results in the different experiments made throughout the study and the data were thus pooled together. Importantly, the FlnA–WT clones produced and studied here were indistinguishable from the original A7 clone.

Previous studies established the critical role of FlnA in the organization of the cortical actin network in M2 cells [8]. Specifically, FlnA-deficient M2 cells exhibited an amoeboid morphology with a prolonged surface blebbing when plated on culture dishes (6 hrs after plating, see arrows in Fig. 2A). On the contrary, neither A7, FlnA–WT, G288R nor P637Q cells exhibited blebs during spreading (Fig. 2A). All the FlnA expressing cells exhibited a mesenchymal-like morphology with cellular protrusions at their periphery. Nevertheless, FlnA–G288R and P637Q expressing cells were smaller than A7 and FlnA–WT cells, both during spreading (6 hours) and at "steady" state (Fig. 2A and B, respectively). Of note, FlnA–WT expressing cells developed more and larger lamellipodia like structures during spreading than G288R and P637Q cells (see arrowheads in Fig. 2A and right-hand histogram in 2B). These observations suggested that actin organization, when compared to that of null cells, was at least partially restored by FlnA mutants during the active remodeling phase of cell spreading. This notion was further corroborated by adhesion kinetic analysis (Xcelligence data below). Also, FlnA localization was not significantly modified by the mutations either and remained co-localized with actin along the cell plasma membranes (Fig. 2C).

To ascertain our observations were not limited to and dependant on the melanoma cells used, another cell model was tested. shRNA FlnA knockdown HT1080 cells were transiently transfected with GFP tagged shRNA-resistant FlnA–WT, G288R and P637Q constructs. As illustrated in Fig. 3A, transient transfection of shRNA resistant filamins restored their expression in HT1080 KO cells. Importantly, as observed in melanoma cells, FlnA–WT transfected cells were larger than mutant FlnA cells during the spreading phase. Also, large lamellipodia were readily observed in FlnA–WT cells and seldom in FlnA–G288R and P637Q mutants (right-hand histogram in Fig. 3B).

Together these data suggest that although the ability of FlnA to organize actin cytoskeleton is maintained in FlnA–G288R and P637Q mutants, the latter may affect actin network during spreading. Because actin dynamics are intimately associated with cell adhesion to a substratum and migration, these properties were analyzed in details.

3.2. FlnA mutations affect cell adhesion and migration capacities

To investigate cell adhesion capacities stably transfected melanoma cells were allowed to adhere for 45 min on fibronectin coated coverslips, the non-adherent cells were then washed away and adherent cells were counted. As shown in Fig. 4A, whereas FlnA–WT expression significantly increased the number of cells adhering in 45 min (x2.4 compared to FlnA–KO (M2) $P < 0.01$ $n = 4$), FlnA mutations did not significantly improve adhesion when compared to the FlnA–KO cells (Fig. 4A).

Cell migration properties were evaluated in Ussing chambers and in wound closure assays. As shown in Fig. 4B, cell migration through a porous filter was significantly increased in only FlnA–WT expressing cells when subjected to a serum gradient ($\times 2.2$ $P < 0.01$ $n = 3$). Similarly, only FlnA–WT cells were able to close a "scratch" made in a confluent cell monolayer within 24 hrs (Fig. 4C).

These data support a mechanism by which FlnA–G288R and P637Q mutations do not significantly affect actin organization and patterning, but do affect overall cell morphology, adhesion, and migration capacities. These data indicate a putative role for these mutations in the activation and remodeling of the actin cytoskeleton. Because small GTPases of the Rho family are key regulators of actin-remodeling reactions governing cell adhesion, migration and morphology, we investigated the influence of these FlnA mutations on RhoA and Rac1 GTPase activities.

3.3. FlnA mutations affect the balance of RhoA–Rac1 activities during spreading

In a first step, we focused on the FlnA–P637Q mutations and performed pull down experiments using GST–Rothekin (GST–RTK) or GST–Cdc42/Rac Interactive Binding (GST–Crib) fusion proteins to evaluate RhoA and Rac1–GTPases activities, respectively. As illustrated in Fig. 5A, Rac1 activity measured in FlnA–P637Q was reduced by more than 50% with respect to that measured for FlnA–WT cells. Conversely, RhoA activity was significantly higher in FlnA–P637Q *vs* FlnA–WT cells (Fig. 5B). To analyze the impact of these small GTPases activities on the kinetics of cell adhesion and spreading, we used the impedance measurement technology of the xCELLigence system. As illustrated in Fig. 6A (left panel), the wild type FlnA "cell index" (CI) rapidly increased after seeding the cells on the E-plate. However, and as expected from the above data, the CI of FlnA–P637Q cells remained lower than that of FlnA–WT cells throughout the experiments. Lower "steady state" CI at 2 hours (before the cells started to divide) corroborated the smaller size of FlnA–P637Q cells we observed (Fig. 2). Also, the slopes of the curves were significantly lower for P637Q *vs* FlnA–WT cells ($dCI/dt = 0.14 \pm 0.02$ CI/min and 0.27 ± 0.03 CI/min, $^{**}P < 0.01$, $n = 4$, respectively). This was consistent with the lower spreading capacities of FlnA–P637Q cells and their lower Rac1 activities. In fact, treatment with the Rac1 specific inhibitor NSC23766 (10 μM) altered the CI of FlnA–WT cells but had no effect on FlnA–P637Q cells (Fig. 6A, left panel). NSC23766 significantly decreased the kinetics and the stationary CI values of FlnA–WT cells down to those of FlnA–P637Q cells. FlnA–WT dCI/dt decreased from 0.27 ± 0.03 CI/min ($n = 4$) to 0.18 ± 0.04 CI/min ($n = 3$, $P < 0.01$) in the presence of 10 μM NSC23766. Values not significantly different from those of FlnA–P637Q cells in the presence and the absence of the inhibitor ($dCI/dt = 0.14 \pm 0.03$ CI/min ($n = 3$) and $dCI/dt = 0.14 \pm 0.02$ CI/min; $n = 4$, respectively).

We then tested the effects of the Rho associated kinase inhibitor (Y27632). In the presence of Y27632 (10 μM), FlnA–P637Q and WT adhesion kinetics were undistinguishable (Fig. 6A, right panel) and both cell lines spread much faster and to a higher extend than untreated FlnA–WT cells ($dCI/dt = 0.44 \pm 0.07$ CI/min and 0.49 ± 0.04 CI/min $n = 4$ non-significant difference, for FlnA–P637Q and WT respectively). Together these data are consistent with a higher RhoA/ROCK signaling activity in FlnA–P637Q cells compared to FlnA–WT expressing cells, which in turn reduces Rac1 activity. This is supported by microscopic observations showing that treatment of FlnA–P637Q cells with Y27632 rescued the cellular morphology and resulted in the de novo formation of large lamellipodia like structures comparable to the WT cells (Fig. 6B). Together, these data support a mechanism by which FlnA–P637Q mutation causes deregulation of the RhoA–Rac1 balance in favor of higher RhoA activity.

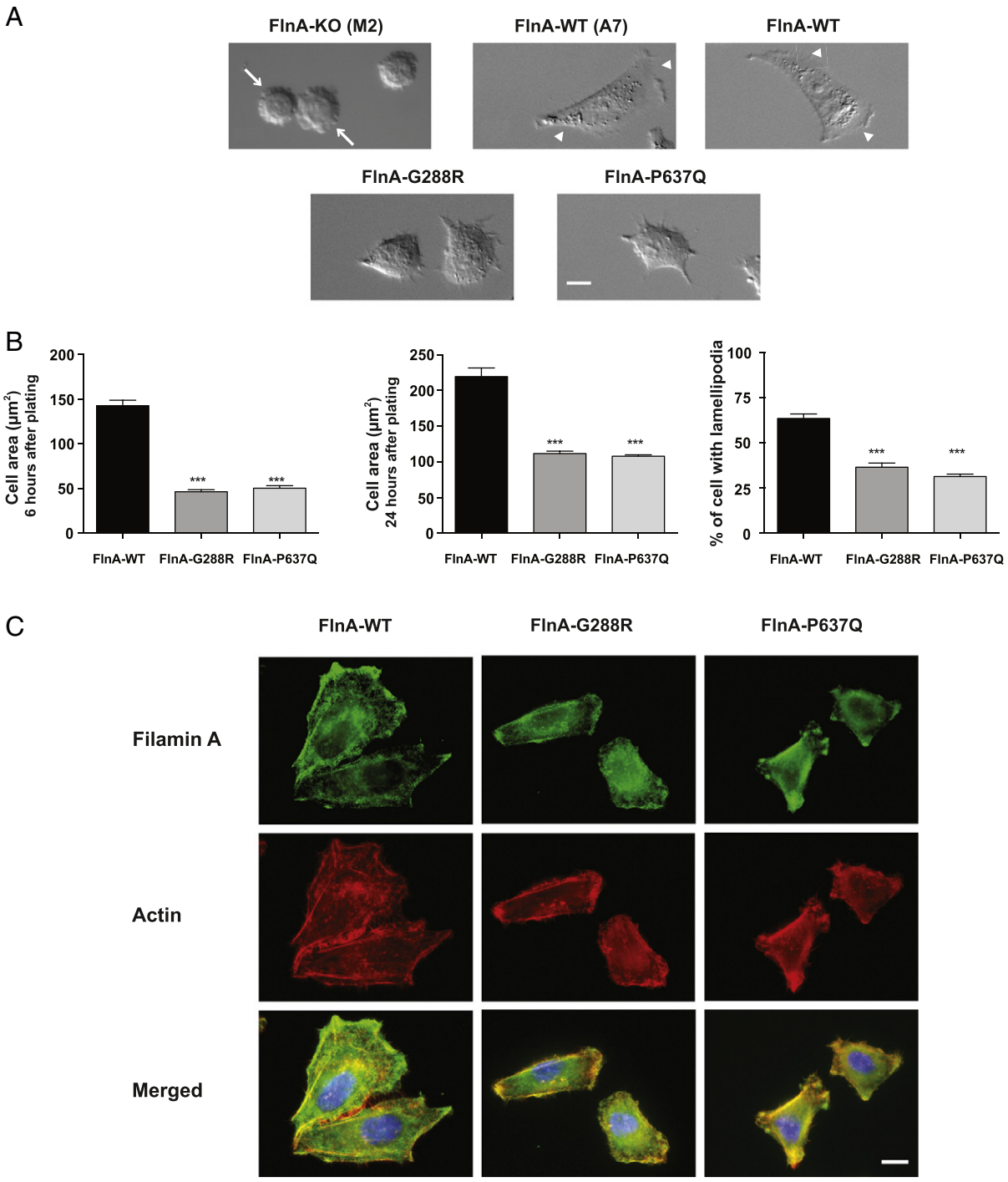

Fig. 2. Filamin A mutations affect cell morphology and size. A. Differential interference contrast images of M2, A7, FlnA–WT, G288R and P637Q cell lines 6 hours after plating. Note the presence of membrane blebs at the surface of FlnA deficient M2 cells only (arrows). A7 and FlnA–WT cells exhibit large lamellipodia structures with membrane ruffles (arrow heads). Scale bar is 10 μm B. Cells expressing FlnA–G288R and P637Q are smaller than FlnA–WT cells. Histograms indicate the area of the cells (μm^2) grown for 6 hrs (left-hand) or 24 hrs (middle). At least 100 cells were measured in 3 experiments. Right-hand histogram indicates the number of cells exhibiting lamellipodia 6 hrs after plating. Error bars show SEM, ***$P < 0.001$ versus FlnA–WT cells. C. Co-localization of FlnA (green) and actin (phalloidin labeling in red) in FlnA–WT, G288R and P637Q cell lines. Note FlnA immunostaining decorates cell plasma membrane. Co-localization of actin and FlnA appears in yellow in the merged images (scale bar 10 μm).

This mechanism also holds for FlnA–G288R cells which exhibited, like FlnA–P637A cells, the same CI features and sensitivity to Rac1 and ROCK inhibitors (NSC23766 and Y27632, Fig. 6C left and right panels, respectively). Importantly, similar adhesion defects of mutant FlnA expressing cells were also observed in shRNA FlnA-knockdown HT1080 cells using the xCELLigence system (Supplementary Fig. S1).

3.4. FlnA FilGAP interactions are not affected by FlnA mutations

Previous studies demonstrated that the reciprocal balance of low Rac1 activity by elevated RhoA/ROCK activity involves GTPase Activating Proteins (GAPs) like ARHGAP22 and a closely related Rac1-specific GAP protein, FilGAP. FilGAP appeared as an interesting candidate

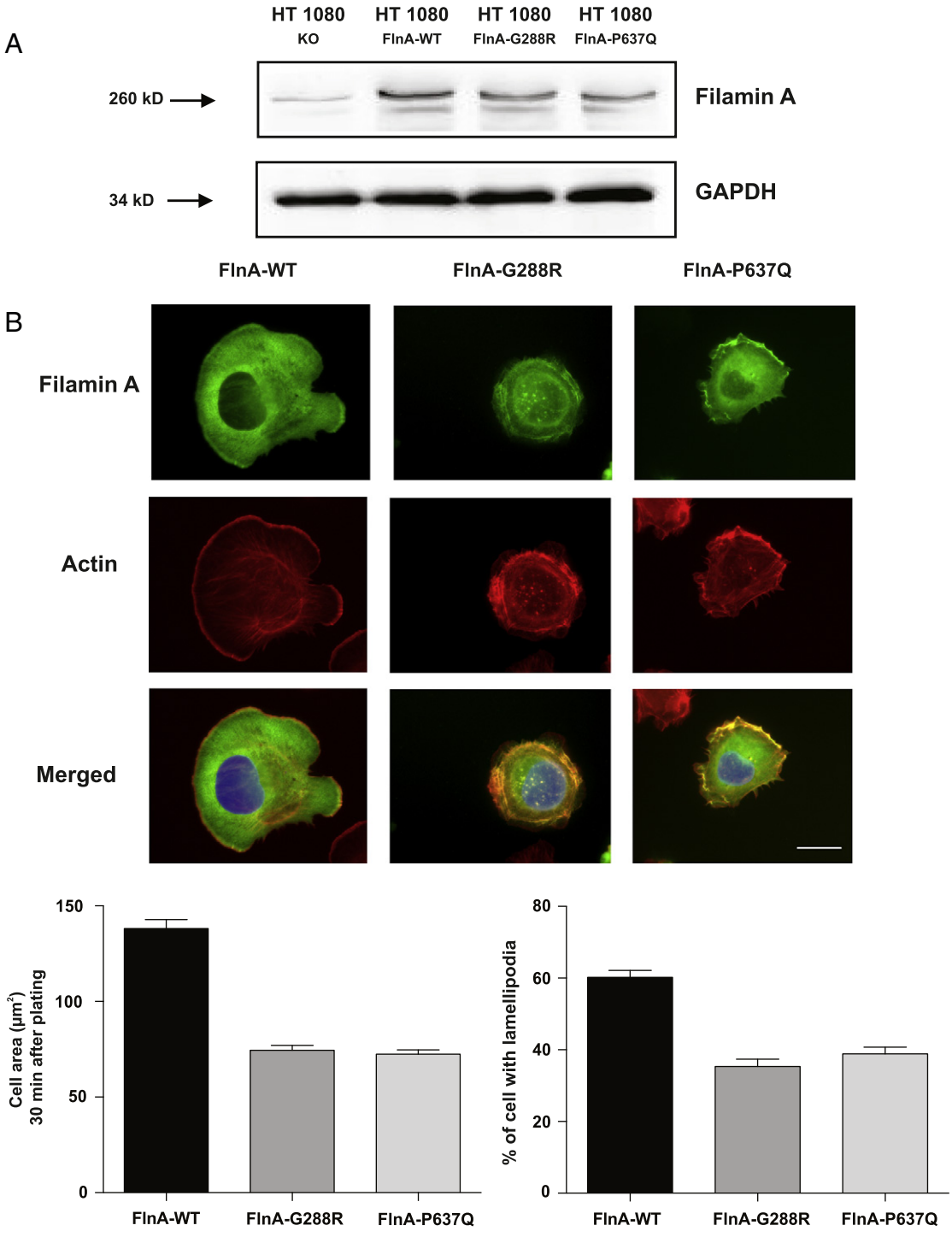

Fig. 3. Filamin A mutations also affect morphology and size of HT1080 cells. A. Western blots of shRNA knockdown FlnA HT1080 cells (first lane) and transfected with shRNA-resistant FlnA–WT, G288R and P637Q. The blot probed with anti-FlnA shows FlnA expression is restored. B. Immuno-localization of GFP-tagged FlnAs using anti-GFP antibody (green) and actin (phalloidin in red, scale bar 10 μm). Cells transfected with mutant FlnA–G288R and P637Q were smaller and exhibited less lamellipodia (left and right-hand histograms, respectively). ***$P < 0.001$ versus FlnA–WT transfected cells ($n = 170$ cells).

because it is known to interact with FlnA and its GAP activity to be regulated by ROCK phosphorylation [26,27]. Indeed, using specific siRNA to silence FilGAP normalized spreading kinetics of both FlnA–P637Q and G288R cells with respect to FlnA–WT cells. As illustrated in Fig. 7A, siRNA treatment efficiently decreased FilGAP expression and FilGAP extinction had a small but significant effect on the early adhesion kinetics of FlnA–WT cells ($dCI/dt = 0.23 \pm 0.05$ *vs* 0.22 ± 0.04 CI/min $n = 4$) but had no effect on steady state CI. On the other hand, consistent with the increased RhoA–ROCK signaling, FilGAP extinction clearly increased both adhesion kinetics and steady state CIs in FlnA–P637Q (from $dCI/dt = 0.12 \pm 0.02$ to 0.19 ± 0.04 CI/min, $n = 4$) and G288R (from $dCI/dt = 0.12 \pm 0.02$ to 0.22 ± 0.03 CI/min, $n = 4$) cells (Fig. 7A, left and right panels respectively). Together these data suggest that increased RhoA–ROCK pathway increases the GAP activity of FilGAP which in turn contributes to imbalanced RhoA–Rac1 activities in FlnA–P637Q and G288R cells and participates in the down regulation of Rac1 during the process of cell attachment. In fact, this idea is consistent with the result of Rac1 GAP activity pull down assays performed

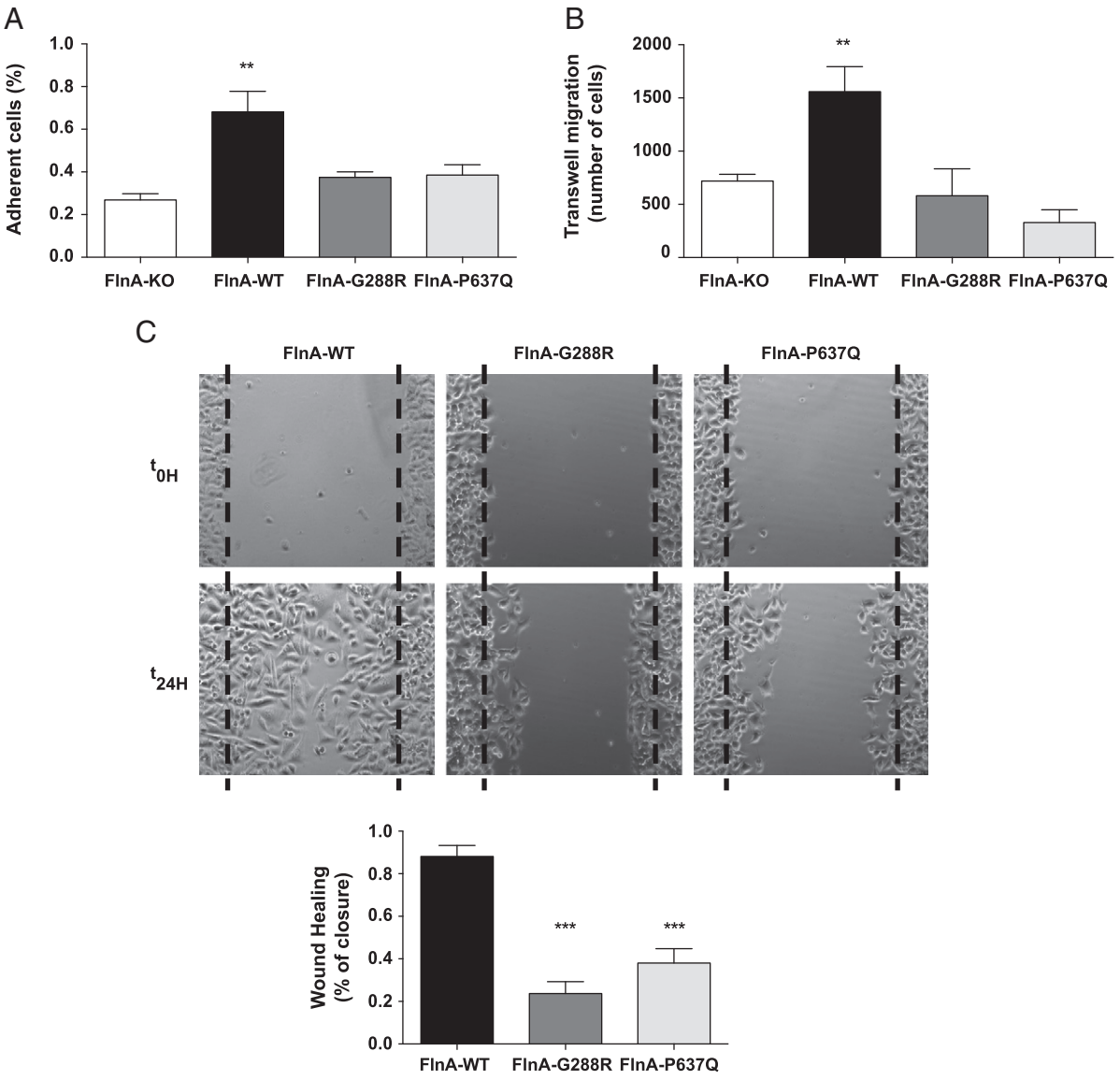

Fig. 4. Filamin A mutations impede cell adhesion and migration. A. Percentage of adherent cells remaining on coverslips coated with fibronectin after two washes. Nuclei were stained with DAPI and counted on 10 fields, $n = 4$, error bars show SEM, $^{**}P < 0.01$ versus FlnA-KO cells. B. Percentage of cells seeded in the upper chamber of "transwell" filters that migrated overnight in the lower chamber. The cells that had migrated were counted on 6 fields from three experiments $n = 3$, error bars show SEM, $^{**}P < 0.01$ versus FlnA-KO (M2) cells. C. Typical images of a wound made at the beginning (t_0) and 24 hrs later ($t_{24\,h}$). Wound healing closure was calculated as the surface of the wound covered by the cells at $t_{24\,h}$ and is expressed in % in the histogram, $n = 3$, error bars show SEM, $^{***}P < 0.001$ versus FlnA–WT cells.

using the constitutively active Rac1–Q61L mutant fused to GST [24]. As shown in Fig. 7C, the amount of "active" FilGAP pulled down from mutant FlnA cell lines more than doubled with respect to that isolated from FlnA–WT cells.

4. Discussion

In the present study, we investigated the effects of FlnA–G288R and P637Q mutations on the actin cytoskeleton organizing properties of FlnA and showed that these point mutations deregulate the balance between RhoA and Rac1 GTPase activities. Our data pointed to an unexpected and new role of the first repeats of FlnA in cell morphology, adhesion and migration capacities.

Since its discovery more than 30 years ago FlnA was identified as an actin binding protein and many studies established its crucial role in actin cytoskeleton remodeling. However, its almost ubiquitous expression and its ability to homo- and hetero-multimerize with FlnB complicated the functional analysis of mutant FlnAs in conventional *in vitro* expression model. In the absence of valvular cellular model easily accessible to experimentation, we chose to use a FlnA-deficient melanoma cell line. Indeed, in their pioneering work Cunningham and colleagues demonstrated that the FlnA deficient cells (M2) used here, exhibit impaired locomotion and develop cell surface blebbing when they attach to and spread on a substratum [8,25]. In M2 cells, intracellular solvent flow drives blebs formation and (re)-expression of exogenous FlnA facilitates actin cortical gelation thereby leading to decreased size and occurrence of the blebs [8]. These observations were consistent with the many studies which, thereafter, highlighted the role of filamin A in cortical actin network organization and stabilization [1–3]. Because, in their original work, Cunningham and colleagues revealed the critical role of the molar FlnA to actin ratio to fully suppress bleb formation and restore M2 cell locomotion, in the present study we a) selected clones with FlnA/actin molar ratios similar to that of the original FlnA–WT expressing cell line (A7) (Fig. 1B) and b) established new FlnA–WT to evaluate possible bias linked to the expression vector and the transfection protocol used. Our data showed that FlnA–WT clones established

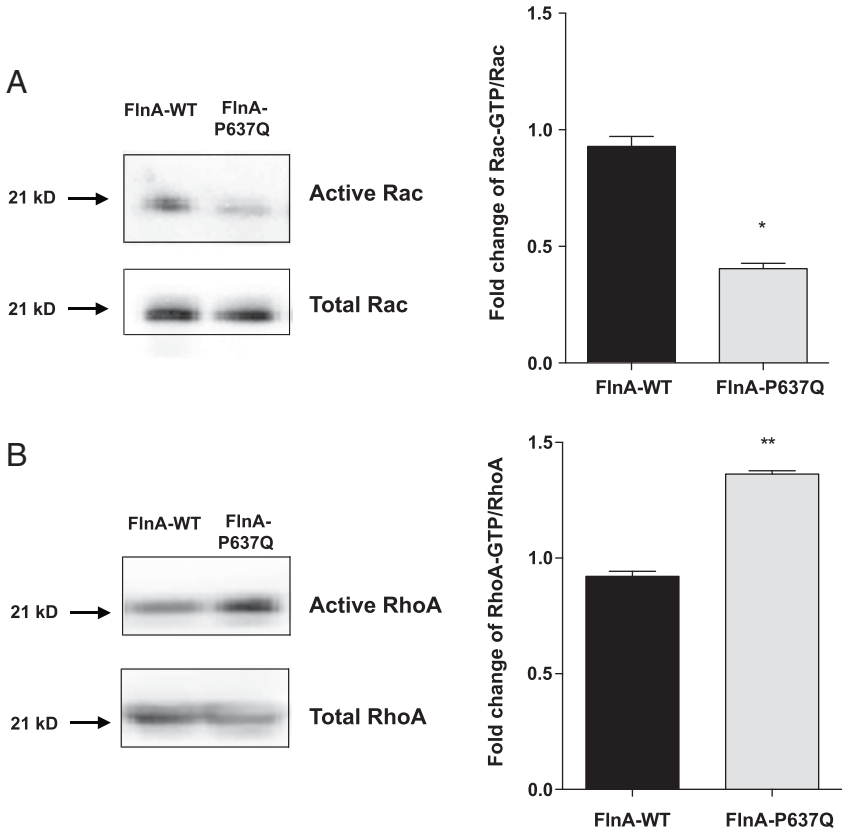

Fig. 5. Rac1 and RhoA GTPases activities are modified in FlnA–P637Q cells. A. Representative experiment of active Rac1 pull down using GST–Crib (left-hand images). Lower Rac1 activity in FlnA–P637Q cells was quantified in five experiments. The mean data are shown on the graph, $n = 4$, Error bars show SEM, $^{*}P < 0.05$. B. Increased RhoA activity was detected in FlnA–P637Q cells (left-hand images). Mean data from five experiments is shown on the graph, Error bars show SEM, $^{**}P < 0.01$ versus FlnA–WT cells.

here were indistinguishable from the original FlnA–WT cell line (A7). Interestingly, FlnA–G288R and P637Q expression also suppressed bleb formation. Together with the absence of any sign of increased protein degradation (not shown) or changes in subcellular localization of mutant FlnAs (Fig. 2) our data indicate that the two mutations do not grossly affect FlnA structure and FlnA–actin interaction. This idea is consistent with the location of the mutations in Igl repeats 1 and 4 of FlnA (for G288R and P637Q, respectively) which are structurally separated from the N-terminal actin binding domain by a hinge and the Igl repeat 9–15 region that constitutes a secondary interaction domain necessary for high avidity binding to F-actin [2,28].

Although physical FlnA–actin interactions are not drastically altered by the mutations, the latter impacted cell spreading and locomotion. Cell migration is known to critically rely on actin cytoskeleton remodeling and many previous studies established the key role of small GTPases Rac1 and RhoA in this process [29,30]. According to a simplistic model, Rac1 is activated at the leading edge of the cells and participates in the formation of lamellipodia and adhesion complexes and thus to forward protrusion. On the other hand, RhoA is inhibited at the leading edge but its activity is then required to stabilize focal adhesion complexes and to activate contractile events like retraction of trailing cell processes that are required for migration. Consistent with this model, we showed the migration-deficient FlnA–P637Q cells exhibited lower Rac1 activity than FlnA–WT cells. Lower Rac1 activities also fit with the observation that the FlnA–G288R and P637Q cells are devoid of lamellipodia-like processes and forward protrusion and they are smaller than FlnA–WT cells. Functional adhesion assays using xCELLigence system further corroborated this notion as Rac1 inhibition using NSC23766 (10 μM) reduced FlnA–WT cells adhesion capacities down to those of FlnA–P637Q and G288R cells. Importantly, similar adhesion defects were also made in another cell model, the HT1080 cells. Because FlnA is known to interact with RhoA and Rac1, one could speculate that the mutations affect their interactions and thus alter their spatial distribution and regulation. Although we did not specifically test mutant-FlnA/GTPases interactions, we suspect this is unlikely because RhoA and Rac1 interaction domains on FlnA are located in C-terminal repeats (Igl 21–23) that are remote from those targeted by the mutations (Igl 1, 4) [30]. Consistent with RhoA activation being required to release the trailing (caudal) regions of the cell from substrates we showed the Rho associated kinase (ROCK) inhibitor (Y27632 10 μM) rescued/stabilized adhesion which correlated with the induction of large lamellipodia like structures in FlnA–P637Q cells. Collectively these data are consistent with a mechanism by which the activated RhoA–ROCK signaling cascade suppresses Rac1 activity resulting in reduced migratory potential.

Mutual antagonism between RhoA and Rac1 GTPases is a well established mechanism that participates to the spatio-temporal regulation of their activities and the Rac1 specific GTPase activating protein FilGAP appeared as an interesting candidate to test. FilGAP is known to bind FlnA and its phosphorylation by ROCK to increase its Rac1–GAP activity [22,26]. Indeed, the Rac–GAP activity assays we performed indicated that "active" FilGAP was significantly increased in mutant FlnA cells compared to FlnA–WT cells (>×2). Together with the rescue of the adhesion of FlnA–P637Q and G288R cells when FilGAP was silenced our data strongly implicate FilGAP in Rac1 down regulation. Preliminary co-immunoprecipitation assays indicate that, although the interactions appeared weaker, mutant FlnAs still bind FilGAP indicating that the mutations do not drastically impair their physical interactions (Supplementary data Fig. S2). Preservation of their interaction is actually consistent with the remote locations of the mutations and FlnA–FilGAP interaction region on FlnA (Igl repeat 1–4 and 23–24, respectively). On

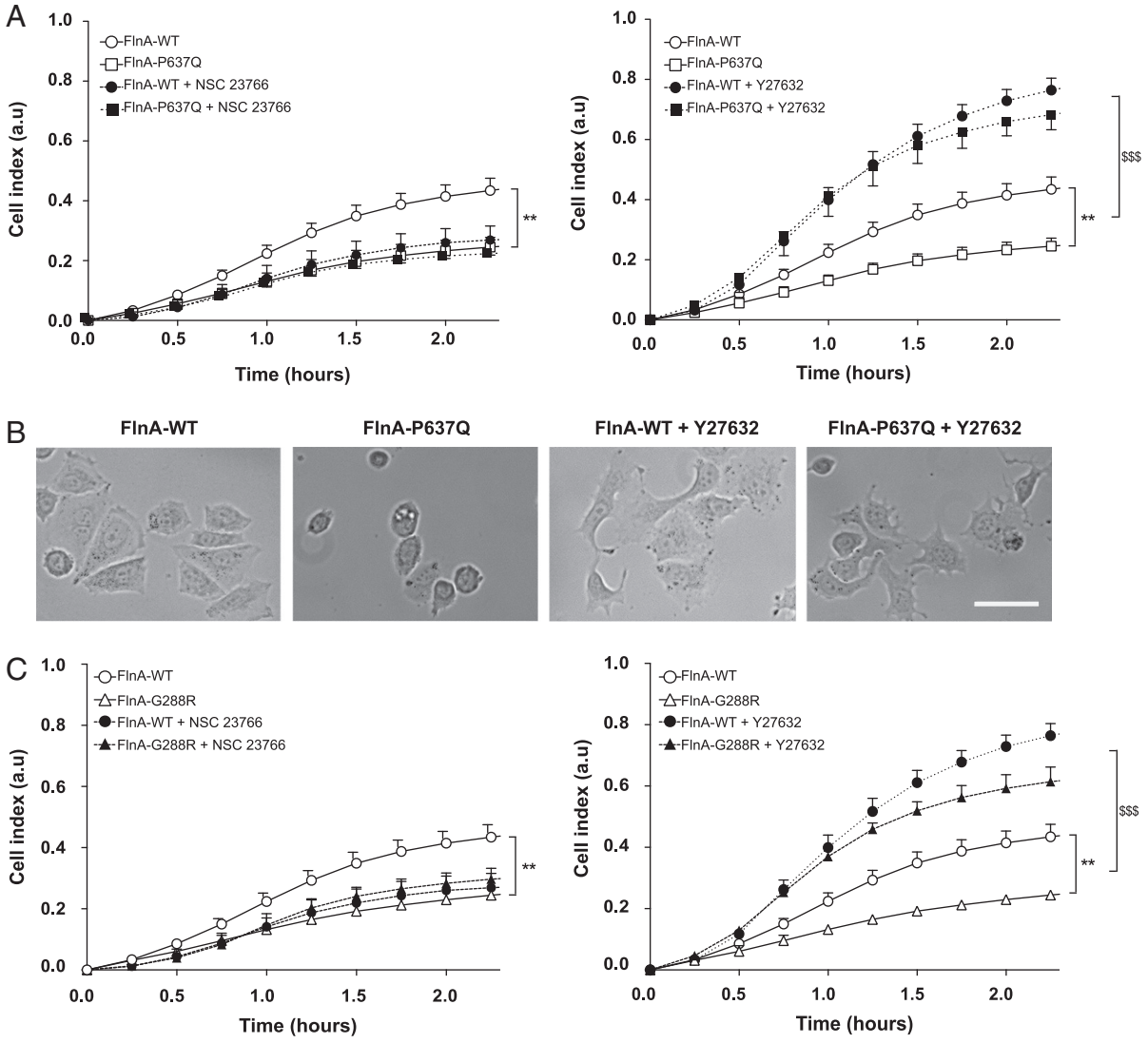

Fig. 6. Rac1 and RhoA activities determine FlnA–P637Q and G288R cells spreading. A. FlnA–WT and P637Q cell indexes (CI) measured using xCELLigence system in the presence and absence of the Rac1 inhibitor NSC23766 (10 μM) in FlnA–P637Q (left panel) and the ROCK inhibitor Y27632 (10 μM). (right panel). FlnA–WT data are included in both panels for comparison. Results are means ± SEM of four independent experiments. ** indicates significant difference between FlnA–WT with and without inhibitors calculated by two-way analysis of variance, Bonferroni corrected testing ($n = 4$, $\$\$\$P < 0.001$ and $^{**}P < 0.01$). B. Phase contrast images of FlnA–WT and FlnA–P637Q cells seeded on fibronectin coverslip (10 μg/ml) for 2 hours with or without Y27632 (10 μM). The inhibitor restores lamellipodia like structure in the mutant cells. Scale bar: 20 μm. C. FlnA–WT and G288R cell indexes (CI) measured using xCELLigence system in the presence and absence of the Rac1 inhibitor NSC23766 (10 μM) in FlnA–P637Q (left panel) and the ROCK inhibitor Y27632 (10 μM) (right panel). FlnA–WT data are included in both panels for comparison. Results are means ± SEM of four independent experiments. ** indicates significant difference between FlnA–WT with and without inhibitor calculated by two-way analysis of variance, Bonferroni corrected testing ($n = 4$, $\$\$\$P < 0.001$ and $^{**}P < 0.01$).

the other hand, our co-immunoprecipitation realized in the absence of mechanical stress may under estimate a potential effect of the mutations on their interaction. In line with the critical role of mechanical strain on FlnA–FilGAP interaction and the prevalence of shear stress and pressure during cardiac contraction, increased FilGAP availability resulting from reduced FlnA–FilGAP interaction might contribute to the pathological process [31]. Future studies will be required to ascertain this issue.

In an effort to elucidate the mechanisms linking FlnA–G288R and P637Q mutations to RhoA activation, we investigated FlnA interaction with R-Ras that was recently shown to bind to the Igl 1–8 repeats region of FlnA [3,9,12]. In addition, Ras effector proteins include guanine nucleotide exchange factors and GTPase-activating proteins such as the Rac1 exchange factor Tiam1, and p120RasGAP/p190RhoGAP complex that couple Ras to RhoA and Rac1 GTPases signaling [32–34]. It was thus tantalizing to speculate that the mutations located in the proximity of R-Ras binding site could alter its binding and Rho–GTPases regulation. However, our preliminary results showed that FlnA–G288R and P637Q mutations do not modify R-Ras binding suggesting FlnA–Ras interaction is not critical to the adhesion and migration deficiencies we observed (Supplementary Fig. S3).

Our data support a mechanism by which specific (N-terminal) FlnA mutations modify actin remodeling pathways. These pathways are critical for cellular responses to mechanical stress, cell–extracellular matrix interactions and epithelial–mesenchymal transformation, three key processes involved in valve development and homeostasis [35]. Interestingly, we recently defined co-operative functional interactions between serotonin, transglutaminase-2 (TG2) and FlnA in the remodeling of cardiac valves during valvulogenesis and "TG2/serotonylation" events participate to actin-remodeling processes and increase RhoA activity [36,37]. Whether small GTPase imbalance and increased RhoA

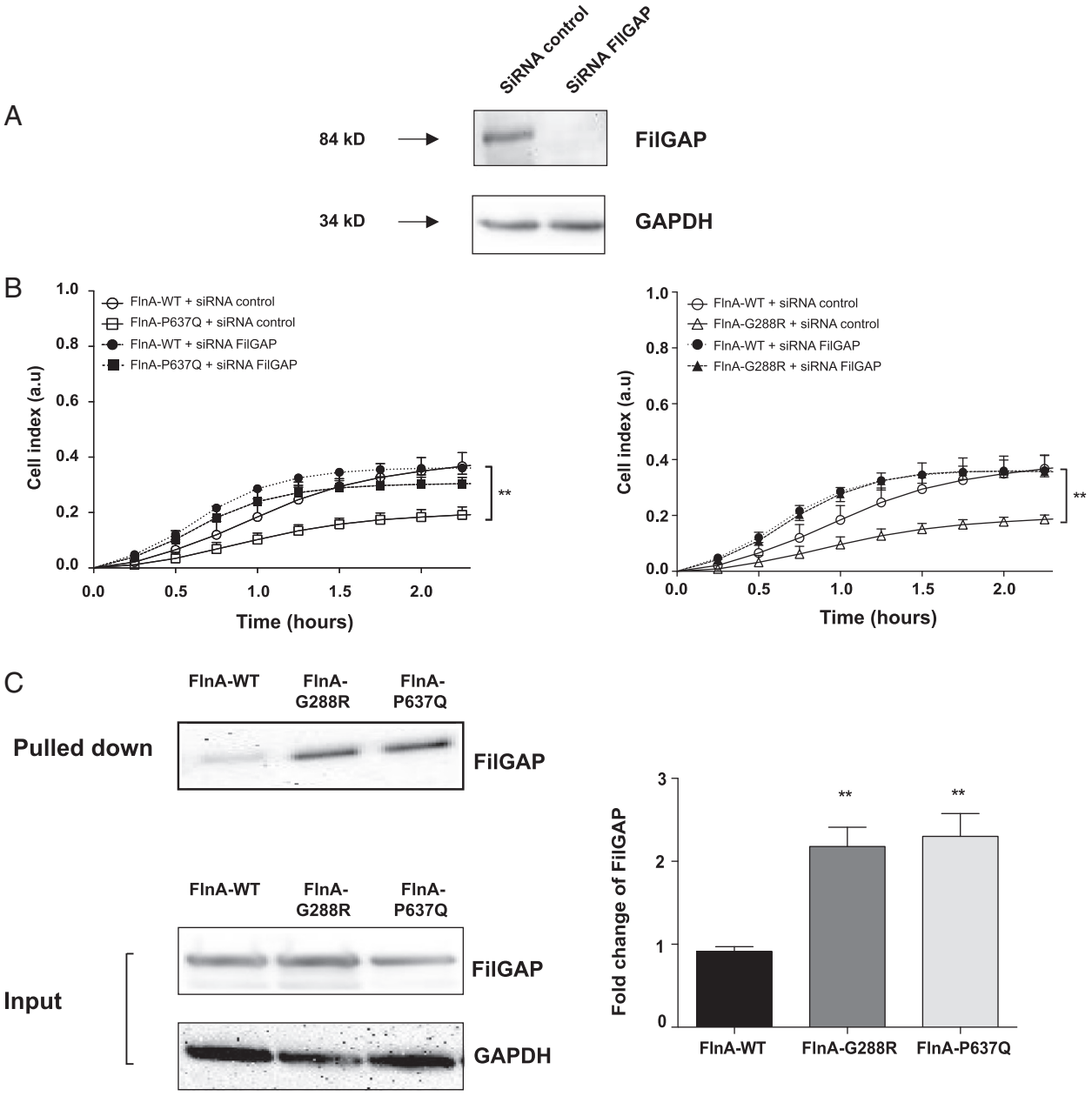

Fig. 7. FilGAP is "activated" and involved in the reduced spreading of FlnA–P637Q and G288R cells. A. Example of FilGAP extinction in FlnA–P637Q cells treated with FilGAP SiRNA. The blot was probed with anti FilGAP and GAPDH (to control loading, 25 μg). B. Cell index of FlnA–P637Q and G288R cells treated with control and FilGAP SiRNA (left and right panels respectively). FlnA–WT data are included in both panels for comparison. Results are means ± SEM of four independent experiments ($n = 4$ Error bars show SEM, $^{**}P < 0.01$.) C. Rac1–GAP activity pull down assay. FlnA–WT, G288R and P637Q melanoma cells were transfected with FilGAP-HA (input lower blot) and "active" FilGAP pulled down using GST–Rac1–Q61L fusion protein (upper blot). "Active" FilGAP pulled down in mutant FlnA cells more than doubled with respect to FlnA–WT cells. $^{**}P < 0.01$ versus FlnA–WT cells ($n = 4$).

serotonylation contribute to valve development and valvular dystrophy remains to be determined [38] but points to candidate therapeutic mechanisms for human heart valve diseases.

Acknowledgments

This work was funded by The Foundation Leducq, Transatlantic Mitral Network of xCELLigence grant 07CVD04 (Paris, France) and the Fédération Française de Cardiologie, Grant R11065NN/RAK1190NNA (TL, JM) (FFC, Paris, France). The work at MUSC was performed in a facility constructed with support from the National Institutes of Health, Grant Number C06 RR018823 from the Extramural Research Facilities Program of the National Center for Research Resources. Other funding sources: National Heart Lung and Blood Institute: R01-HL33756 (RRM), COBRE 1P30 GM103342 (RRM, RAN), 8P20 GM103444 (RRM and RAN); American Heart Association: 11SDG5270006 (RAN); National Science Foundation: EPS-0903795 (RRM); NHLBI K24 HL67434 and HL109506 (RAL).

Appendix A. Supplementary data

Supplementary data to this article can be found online at http://dx.doi.org/10.1016/j.bbamcr.2013.10.022.

References

[1] Y. Feng, C.A. Walsh, The many faces of filamin: a versatile molecular scaffold for cell motility and signalling, Nat. Cell Biol. 6 (2004) 1034–1038.
[2] F. Nakamura, T.M. Osborn, C.A. Hartemink, J.H. Hartwig, T.P. Stossel, Structural basis of filamin A functions, J. Cell Biol. 179 (2007) 1011–1025.

[3] F. Nakamura, T.P. Stossel, J.H. Hartwig, The filamins: organizers of cell structure and function, Cell Adh. Migr. 5 (2011) 160–169.
[4] J.H. Hartwig, J. Tyler, T.P. Stossel, Actin-binding protein promotes the bipolar and perpendicular branching of actin filaments, J. Cell Biol. 87 (1980) 841–848.
[5] T.P. Stossel, J. Condeelis, L. Cooley, J.H. Hartwig, A. Noegel, M. Schleicher, S.S. Shapiro, Filamins as integrators of cell mechanics and signalling, Nat. Rev. Mol. Cell Biol. 2 (2001) 138–145.
[6] A.X. Zhou, J.H. Hartwig, L.M. Akyurek, Filamins in cell signaling, transcription and organ development, Trends Cell Biol. 20 (2010) 113–123.
[7] X. Zhou, J. Boren, L.M. Akyurek, Filamins in cardiovascular development, Trends Cardiovasc. Med. 17 (2007) 222–229.
[8] C.C. Cunningham, Actin polymerization and intracellular solvent flow in cell surface blebbing, J. Cell Biol. 129 (1995) 1589–1599.
[9] A. Lardeux, F. Kyndt, S. Lecointe, H.L. Marec, J. Merot, J.J. Schott, T. Le Tourneau, V. Probst, Filamin-a-related myxomatous mitral valve dystrophy: genetic, echocardiographic and functional aspects, J. Cardiovasc. Transl. Res. 4 (2011) 748–756.
[10] S.S. Ithychanda, D. Hsu, H. Li, L. Yan, D.D. Liu, M. Das, E.F. Plow, J. Qin, Identification and characterization of multiple similar ligand-binding repeats in filamin: implication on filamin-mediated receptor clustering and cross-talk, J. Biol. Chem. 284 (2009) 35113–35121.
[11] H. Kim, F. Nakamura, W. Lee, C. Hong, D. Perez-Sala, C.A. McCulloch, Regulation of cell adhesion to collagen via beta1 integrins is dependent on interactions of filamin A with vimentin and protein kinase C epsilon, Exp. Cell Res. 316 (2010) 1829–1844.
[12] J.E. Gawecka, G.S. Griffiths, B. Ek-Rylander, J.W. Ramos, M.L. Matter, R-Ras regulates migration through an interaction with filamin A in melanoma cells, PLoS One 5 (2010) e11269.
[13] G.S. Griffiths, M. Grundl, J.S. Allen III, M.L. Matter, R-Ras interacts with filamin a to maintain endothelial barrier function, J. Cell. Physiol. 226 (2011) 2287–2296.
[14] H. Falet, A.Y. Pollitt, A.J. Begonja, S.E. Weber, D. Duerschmied, D.D. Wagner, S.P. Watson, J.H. Hartwig, A novel interaction between FlnA and Syk regulates platelet ITAM-mediated receptor signaling and function, J. Exp. Med. 207 (2010) 1967–1979.
[15] H. Kim, F. Nakamura, W. Lee, Y. Shifrin, P. Arora, C.A. McCulloch, Filamin A is required for vimentin-mediated cell adhesion and spreading, Am. J. Physiol. Cell Physiol. 298 (2010) C221–C236.
[16] S.P. Robertson, Z.A. Jenkins, T. Morgan, L. Ades, S. Aftimos, O. Boute, T. Fiskerstrand, S. Garcia-Minaur, A. Grix, A. Green, V. Der Kaloustian, R. Lewkonia, B. McInnes, M.M. van Haelst, G. Mancini, T. Illes, G. Mortier, R. Newbury-Ecob, L. Nicholson, C.I. Scott, K. Ochman, I. Brozek, D.J. Shears, A. Superti-Furga, M. Suri, M. Whiteford, A.O. Wilkie, D. Krakow, Frontometaphyseal dysplasia: mutations in FLNA and phenotypic diversity, Am. J. Med. Genet. A 140 (2006) 1726–1736.
[17] V.L. Sheen, P.H. Dixon, J.W. Fox, S.E. Hong, L. Kinton, S.M. Sisodiya, J.S. Duncan, F. Dubeau, I.E. Scheffer, S.C. Schachter, A. Wilner, R. Henchy, P. Crino, K. Kamuro, F. DiMario, M. Berg, R. Kuzniecky, A.J. Cole, E. Bromfield, M. Biber, D. Schomer, J. Wheless, K. Silver, G.H. Mochida, S.F. Berkovic, F. Andermann, E. Andermann, W.B. Dobyns, N.W. Wood, C.A. Walsh, Mutations in the X-linked filamin 1 gene cause periventricular nodular heterotopia in males as well as in females, Hum. Mol. Genet. 10 (2001) 1775–1783.
[18] V.L. Sheen, A. Jansen, M.H. Chen, E. Parrini, T. Morgan, R. Ravenscroft, V. Ganesh, T. Underwood, J. Wiley, R. Leventer, R.R. Vaid, D.E. Ruiz, G.M. Hutchins, J. Menasha, J. Willner, Y. Geng, K.W. Gripp, L. Nicholson, E. Berry-Kravis, A. Bodell, K. Apse, R.S. Hill, F. Dubeau, F. Andermann, J. Barkovich, E. Andermann, Y.Y. Shugart, P. Thomas, M. Viri, P. Veggiotti, S. Robertson, R. Guerrini, C.A. Walsh, Filamin A mutations cause periventricular heterotopia with Ehlers–Danlos syndrome, Neurology 64 (2005) 254–262.
[19] J.A. Bernstein, D. Bernstein, U. Hehr, L. Hudgins, Familial cardiac valvulopathy due to filamin A mutation, Am. J. Med. Genet. A 155A (2011) 2236–2241.
[20] F. Kyndt, J.P. Gueffet, V. Probst, P. Jaafar, A. Legendre, F. Le Bouffant, C. Toquet, E. Roy, L. McGregor, S.A. Lynch, R. Newbury-Ecob, V. Tran, I. Young, J.N. Trochu, H. Le Marec, J.J. Schott, Mutations in the gene encoding filamin A as a cause for familial cardiac valvular dystrophy, Circulation 115 (2007) 40–49.
[21] M. Baldassarre, Z. Razinia, C.F. Burande, I. Lamsoul, P.G. Lutz, D.A. Calderwood, Filamins regulate cell spreading and initiation of cell migration, PLoS One 4 (2009) e7830.
[22] K. Saito, Y. Ozawa, K. Hibino, Y. Ohta, FilGAP, a Rho/Rho-associated protein kinase-regulated GTPase-activating protein for Rac, controls tumor cell migration, Mol. Biol. Cell 23 (2012) 4739–4750.
[23] R.J. Keogh, New technology for investigating trophoblast function, Placenta 31 (2010) 347–350.
[24] C. Guilluy, A.D. Dubash, R. Garcia-Mata, Analysis of RhoA and Rho GEF activity in whole cells and the cell nucleus, Nat. Protoc. 6 (2011) 2050–2060.
[25] C.C. Cunningham, J.B. Gorlin, D.J. Kwiatkowski, J.H. Hartwig, P.A. Janmey, H.R. Byers, T.P. Stossel, Actin-binding protein requirement for cortical stability and efficient locomotion, Science 255 (1992) 325–327.
[26] Y. Ohta, J.H. Hartwig, T.P. Stossel, FilGAP, a Rho- and ROCK-regulated GAP for Rac binds filamin A to control actin remodelling, Nat. Cell Biol. 8 (2006) 803–814.
[27] F. Nakamura, FilGAP and its close relatives: a mediator of Rho-Rac antagonism that regulates cell morphology and migration, Biochem. J. 453 (2013) 17–25.
[28] G.M. Sawyer, A.J. Sutherland-Smith, Crystal structure of the filamin N-terminal region reveals a hinge between the actin binding and first repeat domains, J. Mol. Biol. 424 (2012) 240–247.
[29] V. Sanz-Moreno, G. Gadea, J. Ahn, H. Paterson, P. Marra, S. Pinner, E. Sahai, C.J. Marshall, Rac activation and inactivation control plasticity of tumor cell movement, Cell 135 (2008) 510–523.
[30] Y. Ohta, N. Suzuki, S. Nakamura, J.H. Hartwig, T.P. Stossel, The small GTPase RalA targets filamin to induce filopodia, Proc. Natl. Acad. Sci. U. S. A. 96 (1999) 2122–2128.
[31] A.J. Ehrlicher, F. Nakamura, J.H. Hartwig, D.A. Weitz, T.P. Stossel, Mechanical strain in actin networks regulates FilGAP and integrin binding to filamin A, Nature 478 (2011) 260–263.
[32] J.M. Lambert, Q.T. Lambert, G.W. Reuther, A. Malliri, D.P. Siderovski, J. Sondek, J.G. Collard, C.J. Der, Tiam1 mediates Ras activation of Rac by a PI(3)K-independent mechanism, Nat. Cell Biol. 4 (2002) 621–625.
[33] A.S. Nimnual, B.A. Yatsula, D. Bar-Sagi, Coupling of Ras and Rac guanosine triphosphatases through the Ras exchanger Sos, Science 279 (1998) 560–563.
[34] S. Schubbert, K. Shannon, G. Bollag, Hyperactive Ras in developmental disorders and cancer, Nat. Rev. Cancer 7 (2007) 295–308.
[35] R.B. Hinton, K.E. Yutzey, Heart valve structure and function in development and disease, Annu. Rev. Physiol. 73 (2011) 29–46.
[36] K. Sauls, A. de Vlaming, B.S. Harris, K. Williams, A. Wessels, R.A. Levine, S.A. Slaugenhaupt, R.L. Goodwin, L.M. Pavone, J. Merot, J.J. Schott, T. Le Tourneau, T. Dix, S. Jesinkey, Y. Feng, C. Walsh, B. Zhou, S. Baldwin, R.R. Markwald, R.A. Norris, Developmental basis for filamin-A-associated myxomatous mitral valve disease, Cardiovasc. Res. 96 (2012) 109–119.
[37] C. Guilluy, M. Rolli-Derkinderen, P.L. Tharaux, G. Melino, P. Pacaud, G. Loirand, Transglutaminase-dependent RhoA activation and depletion by serotonin in vascular smooth muscle cells, J. Biol. Chem. 282 (2007) 2918–2928.
[38] R.A. Norris, R. Moreno-Rodriguez, A. Wessels, J. Merot, P. Bruneval, A.H. Chester, M.H. Yacoub, A. Hagege, S.A. Slaugenhaupt, E. Aikawa, J.J. Schott, A. Lardeux, B.S. Harris, L.K. Williams, A. Richards, R.A. Levine, R.R. Markwald, Expression of the familial cardiac valvular dystrophy gene, filamin-A, during heart morphogenesis, Dev. Dyn. 239 (2010) 2118–2127.